MAPPING OF HDO AND H_2O IN THE MARTIAN ATMOSPHERE. R. E. Novak[1], M. J. Mumma[2], G. Villanueva[2], B. Bonev[3], and M. DiSanti[2]; [1]Iona College, New Rochelle, N.Y. 10801 (rnovak@iona.edu), [2]Code 690 NASA GSFC, Greenbelt, MD 20771-0003, (Michael.j.mumma@nasa.gov, villanueva@ssedmail.gsfc.nasa.gov, disanti@ssedmail.gsfc.nasa.gov), [3]Catholic University of America, Washington D.C., 20064-0001 and NASA GSFC (bbonev@ssedmail.gsfc.nasa.gov).

Introduction: We report investigations of HDO and H_2O on Mars using CSHELL at the NASA IRTF for seasonal dates that span the entire Mars year. Our objective is to obtain measurements of the seasonal and latitudinal variation of the [HDO]/[H_2O] ratio and thereby obtain better insights into the dynamics of Mars' atmosphere. The instrument slit is typically positioned N-S along the central meridian resulting in a one-dimensional map of HDO (1997-2006) and/or H_2O (2001-2006) [1]. Column densities are extracted at intervals between 0.6 and 1.0 arc-second; [HDO]/[H_2O] ratios are calculated for various latitudes and seasons. Our database includes seasonal dates in Table I.

TABLE I
CSHELL Observations of Mars

UT Date	L_s	Del-Dot (km sec^{-1})	Diameter arc-sec
21-Jan-97	67.3°	-15.3	9.6
10-Jan-02	306.0°	+13.0	6.0
13-Jan-03	124.0°	-14.9	4.8
21-Mar-03	154.7°	-15.6	6.9
15-Jan-07	357.2°	+16.3	10.3

The values for the [HDO]/[H_2O] ratio on Mars are useful in developing atmospheric models, estimating the evolution of water on Mars, and dating Mars meteorites [2,3,4,5,6]. We have measured ratios approximately five times larger than the Standard Mean Ocean Water (SMOW) ratio on earth; we have found this ratio to vary with season and latitude [7]. The [HDO]/[H_2O] ratio is believed to have increased over time through Rayleigh distillation [3,4]. The efficiency of deuterium to hydrogen escape is 32% for the present epoch [4]. Also, the ratio could display a hemispherical variation because of different mean temperatures in the polar caps.

Observations: Our group has initiated an observing program to test the hypothesis that the polar caps have different concentrations of HDO [8]. We conduct nearly simultaneous measurements of HDO and H_2O in the near-IR. DiSanti and Mumma developed a technique for mapping HDO on Mars through its ν_1 fundamental band near 3.67 μm using CSHELL at the NASA IRTF [9]. Novak et al. extended the approach significantly and describe nearly simultaneous measurements of ozone and HDO on Mars acquired in January 1997 ($L_s = 67^o$) [1]. For data taken from 1997 to 2003, we compared our HDO data to H_2O results obtained from TES [10] (M. Smith, private communication). Since 2003, we have been using absorption lines near 3.33 μm to determine H_2O abundances. The approach is illustrated in Figure 1 with data taken on January 15, 2006 when $L_s = 357^o$.

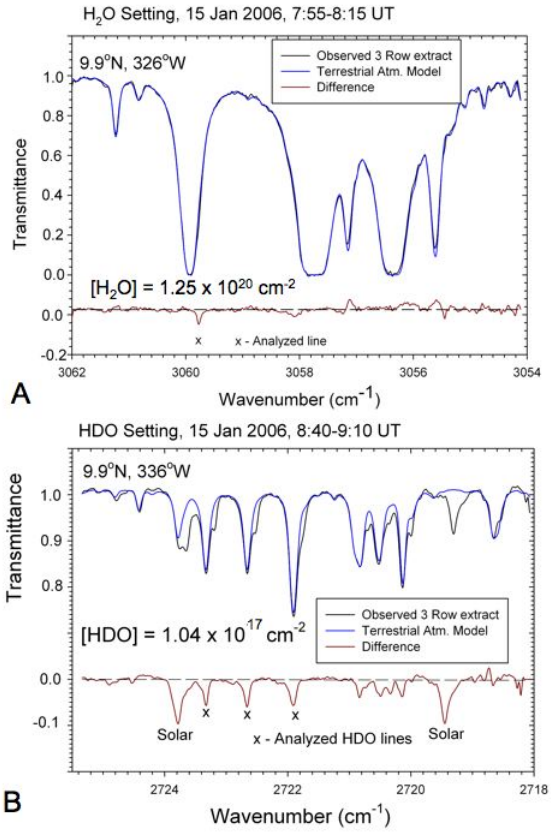

Fig. 1. Detection of HDO (top panel) and H_2O (lower panel) for January 15, 2006, $L_s = 357^o$. The slit was N-S on Mars and the spectra/spatial images were integrated for four minutes on Mars. Top traces are observed spectral extracts (3 rows or 0.6 arc-second). The spectral lines on Mars are Doppler shifted from their terrestrial counterparts (+16.3 km/sec). Terrestrial models were constructed and subtracted from the observed spectra.

The difference appears in the lower traces. A best-fit Mars model provides the measured column density. H_2O spectra were also taken near 3028 and 3035 cm^{-1}.

Analysis: The spectra were analyzed by generating models for both Mar's and the Earth's atmosphere. GENLN2 [11], a line-by-line atmospheric transmittance and radiance model, was used to construct these models. GENLN2 uses a twenty-nine layer profile of the atmosphere (pressure, temperature, and molecular density values for each layer) with spectral lines from the HITRAN-2004 database [12]. First, a model of the Earth's atmosphere was constructed to fit the terrestrial lines of the observed spectra (Fig. 1). This model was subtracted from the observed spectra resulting in residuals containing the Mars absorptions (lower traces in Fig. 1). Using a similar layered profile for the Martian atmosphere, a Mars model was constructed and Doppler shifted (Fig. 2). This model was combined with the Earth model; then the Earth model was subtracted from the combined model to obtain a model for the residuals (lowest trace, Fig. 2).

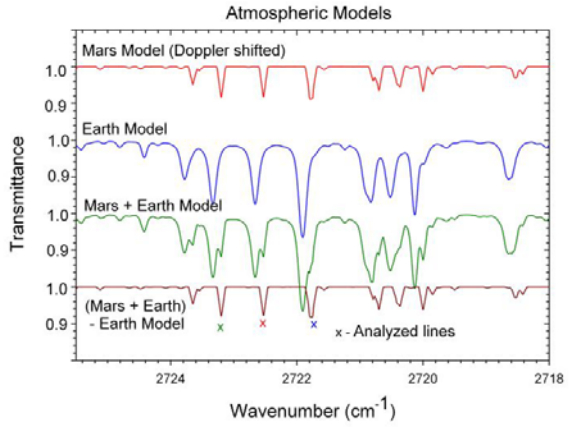

Fig 2. Atmospheric models generated by GENLN2. Such models are used to determine molecular column densities from spectral extracts as presented in Fig. 1. A Mars model consisting of vertical profiles of temperature, pressure, and molecular densities in twenty-nine layers is first constructed; it is then shifted according to its relative velocity with the earth and sun. Similarly, a best fit model is generated for the Earth's atmosphere and combined with the Mar's model. The Earth model is then subtracted from the combined model to obtain the remaining Mars lines. A best fit is performed between the difference spectra of the model and the observation. The model is constructed using the natural line widths, and is deconvolved to the CSHELL resolution (~40000).

The temperature of Mars' surface and atmosphere changes with latitude. The spectral continuum observed is a combination of reflected sunlight and thermal emission from Mars; the relative component of each is obtained by measuring the equivalent width of the observed solar Fraunhofer lines (Fig. 1b) [1]. As the thermal emission increases, the observed equivalent width decreases. The relative size of the absorption lines in the HDO spectra (indicated by x's in Figs. 1b and 2) changes with temperature. Our Mars model includes the thermal emission and the temperature profile of the atmosphere. The column densities reported are those that have the best fit to the observed spectra.

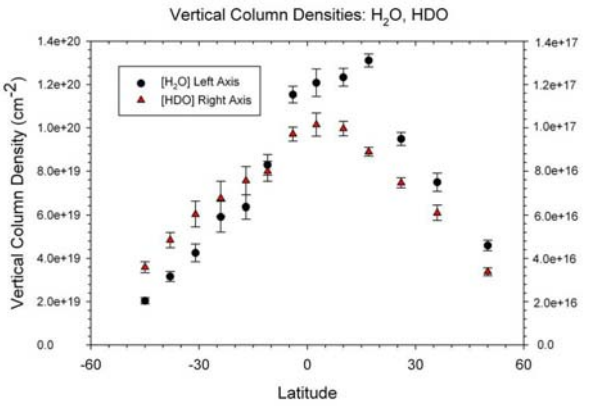

Fig. 3. Measured column densities for H_2O and HDO on 15 January 2006 ($L_s = 357^o$). The H_2O values are consistent with TES values for the same season [10]. Note that in the southern hemisphere 1000*[HDO] is greater than [H_2O] whereas in the northern hemisphere, the relative values are reverse. A similar pattern has been reported for data taken at $L_s = 67^o$ [8].

Results: Our measurements of H_2O and HDO column densities for data taken at $L_s = 357^o$ appear in Fig. 3. The ratio of these values compared to SMOW appears in Fig. 4a. At this season, dust and ice clouds in the atmosphere are at a minimum [10]. Also appearing in Fig. 4 are previously reported values of [HDO]/[H_2O] ratio [8]. The [HDO] values are from our analysis of CSHELL data; the [H_2O] values are from TES taken at the same season but different years. The [HDO]/[H_2O] ratio for $L_s = 357^o$ in the northern hemisphere is constant with latitude and lower than previously measured values; the northern hemisphere is coming out of winter when much of the water vapor in the atmosphere has condensed into ice. Since HDO preferentially condenses before H_2O, we believe that the ratio would be lower than at other seasons. In the southern hemisphere, the ratio increases southward. This pattern also appears with our results from $L_s = 67^o$ [8], but the ratios are higher in both hemispheres.

Water vapor in the northern hemisphere drastically increases between $L_s = 357^o$ and $L_s = 67^o$ [10]. At $L_s = 67^o$, most of the water vapor in the atmosphere would have been recently sublimated from the ice in the polar cap which could explain the higher [HDO]/[H_2O] ratio. Fig. 4b shows data from both seasons normalized to the [HDO]/[H_2O] ratio in the northern hemisphere and plotted with respect to the latitude from the sub-solar point. The "normalized" ratios for the two seasons are consistent with each other. Both show an increase in the ratio towards the south.

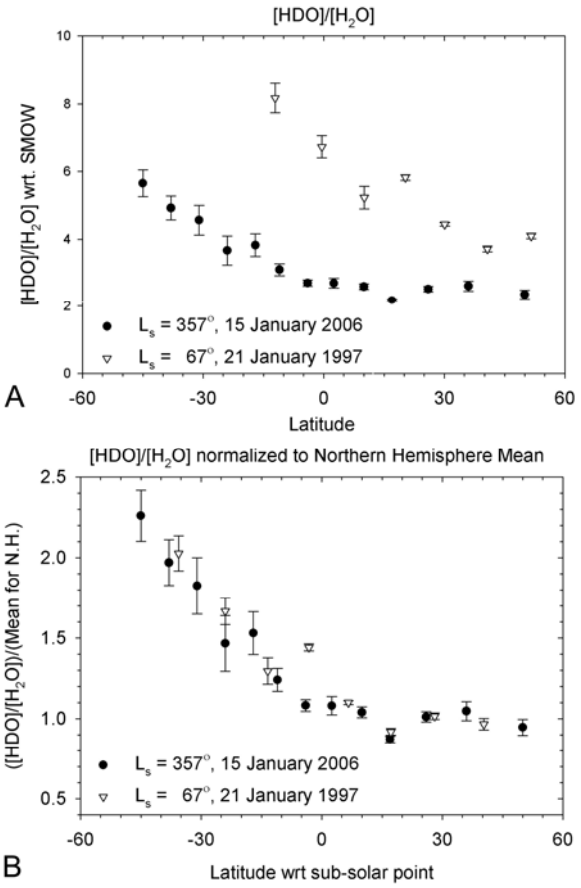

Fig. 4. Results for $L_s = 357^o$ compared to data taken for $L_s = 67^o$. **A.** The ratio for $L_s = 67^o$ was obtained with our results [1] and the H_2O values were taken from the TES database (M. Smith, private communication) for the same season but successive Martian years [8]. The $L_s = 357^o$ values were obtained from data presented in Fig. 3. **B**. The results of Fig. 4a are normalized to their mean values in the northern hemisphere and plotted with respect to latitudes relative to the sub-solar point (23.5^oN for $L_s = 67^o$; 1^oS for $L_s = 357^o$). For both sets of data, the ratio north of the sub-solar latitude is relatively constant, but their means differ, probably because of seasonal effects. Likewise, the ratio increases towards the south.

Conclusions: Both set of results indicate a larger [HDO]/[H_2O] ratio in the southern hemisphere; preliminary analysis of data for the other dates presented in Table I show a similar pattern [7]. We conclude that deuterium is preferentially sequestered in the southern polar cap. Montmessin's model [5] predicts a constant value from 30^oS to 30^oN with a decrease approaching the polar regions. Fisher's model [6] uses different ground reservoirs and has developed scenarios for a hemispherical variation of the [HDO]/[H_2O] ratio. These and other models that explain the [HDO]/[H_2O] ratio are based on relatively few observations. Our measurements will help to perfect these models.

We will reanalyze our observations for the other seasonal dates presented in Table I using recently developed analysis techniques. The GENLN2 atmospheric model has enabled us to model more accurately the Earth's atmosphere, thus providing better measurements of the Mars absorptions. Observations of Mars for northern spring, when the water vapor content of both hemispheres rapidly changes, have been proposed for the near future.

Acknowledgements: This work was support in parts by grants from NASA (RTOP 344-32-30-10) and the NSF (AST-0505765). We also thank the NASA-IRTF for telescope time and staff support.

References : [1] Novak, R.E., et al. (2002), *Icarus*,**158**,14-23. [2] Hunten, D.M. (1974), *Rev. Geophys. Space Phys.*, **12**,529-535. [3] Krasnoplosky, V.A., (1993), *Icarus*, **101**,313-332. [4] Yung, Y.L. and W.B. DeMore (1999), *Photochemistry of Planetary Atmospheres*, (Oxford University Press, New York). [5] Montmessin, F. et al., (2005), *J. Geophys. Res*, **110**, E03006. [6] Fisher, D.A., (2007), *Icarus*, **187**, 430-441. [7] Novak R. E, et al, (2006), *B.A.A.S.*, **38**, 625. [8] Mumma, M.J., et al.(2003), Sixth International Conference on Mars, Abstract # 3186. [9] DiSanti, M.A. and M.J. Mumma, (1995), *Workshop on Mars Telescope Observations* (Cornell U. Press). [10] Smith, M.D., (2007), *Icarus*,**167**,148-165. [11] Edwards, D. (1992), GENLN2:Description and Users Guide (technical report), NCAR, Boulder. [12] Rothman, L. et al., (2005), *J. of Quan. Spec.Rad.Tran.*, **96**, 139-204.